

SEMIOCCAM: A ROBUST SEMI-SUPERVISED IMAGE RECOGNITION NETWORK USING SPARSE LABELS

Rui Yann* 

Shu1L0n9@gmail.com

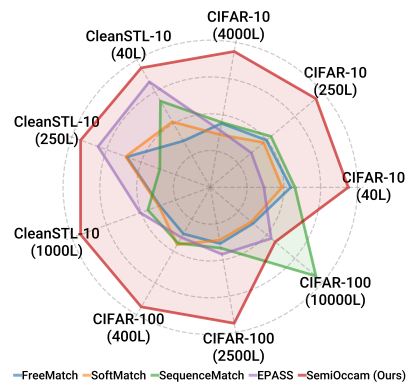
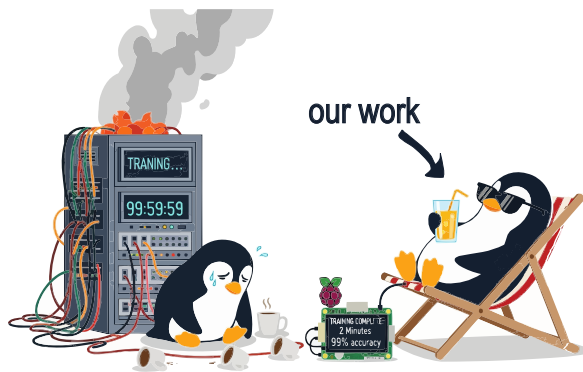
Tianshuo Zhang 

zhang.tianshuo@163.com

Xianglei Xing† 

xingxl@hrbeu.edu.cn

General Artificial Intelligence Laboratory
College of Intelligent Systems Science and Engineering
Harbin Engineering University
Harbin, 150001, China



ABSTRACT

We present **SemiOccam**, an image recognition network that leverages semi-supervised learning in a highly efficient manner. *Existing works* often rely on complex training techniques and architectures, *requiring hundreds of GPU hours for training*, while their *generalization ability* when dealing with extremely limited labeled data *remains to be improved*. To address these limitations, we construct a hierarchical mixture density classification decision mechanism by **optimizing mutual information** between feature representations and target classes, compressing redundant information while retaining crucial discriminative components. Experimental results demonstrate that our method achieves **state-of-the-art performance** on **three commonly used datasets**, with accuracy **exceeding 95%** on two of them, using **only 4 labeled samples per class**, and its simple architecture **keeps training time to minute-level**. Notably, this paper **reveals a long-overlooked data leakage issue** in the STL-10 dataset for semi-supervised learning tasks and removes duplicates to ensure the reliability of experimental results. We also release the deduplicated CleanSTL-10 dataset to **facilitate fair and reliable research** in future semi-supervised learning.¹²

Keywords: Semi-Supervised Learning, Image Recognition, Vision Transformer, Gaussian Mixture Model

*Rui performed this research during an internship.

†Corresponding author.

¹Code available at <https://github.com/Shu1L0n9/SemiOccam>.

²CleanSTL-10 available at <https://huggingface.co/datasets/Shu1L0n9/CleanSTL-10>.

1 INTRODUCTION

Deep learning has achieved remarkable success in image classification tasks. However, its performance is **highly dependent** on large-scale annotated datasets. In real-world applications, labeled data is often scarce and **expensive to acquire**. Therefore, semi-supervised learning (SSL) has received widespread attention in recent years as an effective solution. The goal of SSL is to train models using a small amount of labeled data and large amount of unlabeled data, thereby improving the model’s generalization ability. Nevertheless, most existing SSL methods, such as consistency regularization and pseudo-labeling, rely on **complex training strategies and network designs**, leading to **training costs of hundreds of GPU hours** [27][39][33] even on high-performance computing resources like NVIDIA V100, and their **generalization ability when labeled data are extremely limited still needs improvement**. Moreover, although some recent works have explored Vision Transformers (ViT) in SSL [40], they have yet to fully exploit its advantages.

The inspiration for this research stems from the **principle of Occam’s razor**. This principle posits that among competing hypotheses that explain the data well, the simplest one is preferred. This motivates us to design a solution that balances model complexity and interpretability, ensuring efficient and effective feature representation while preventing unnecessary overfitting.

Aligned with this ethos, we delve into Gaussian Mixture Models (GMM), powerful probabilistic models that assume data is generated from a mixture of multiple Gaussian distributions. This exploration also draws from the systematic study by Miller & Uyar on the “Mixture of Experts (MoE)” structure based on the joint probability model of features and labels. In our research, we found that the performance of GMM is highly related to the quality of feature vectors. If the features lack representativeness or have insufficient discriminative power, the classification performance will be severely affected.

To address this, we designed a feature encoding framework based on a self-attention mechanism to fully exploit the global contextual information in images and generate more discriminative feature representations. This enhanced feature quality is crucial for optimizing MoE classifier’s performance. **Furthermore**, to effectively leverage large amounts of unlabeled data, we incorporated a semi-supervised learning strategy utilizing a pseudo-labeling mechanism. An overview of our network, illustrating the integration of these approaches, is provided in Figure 1.

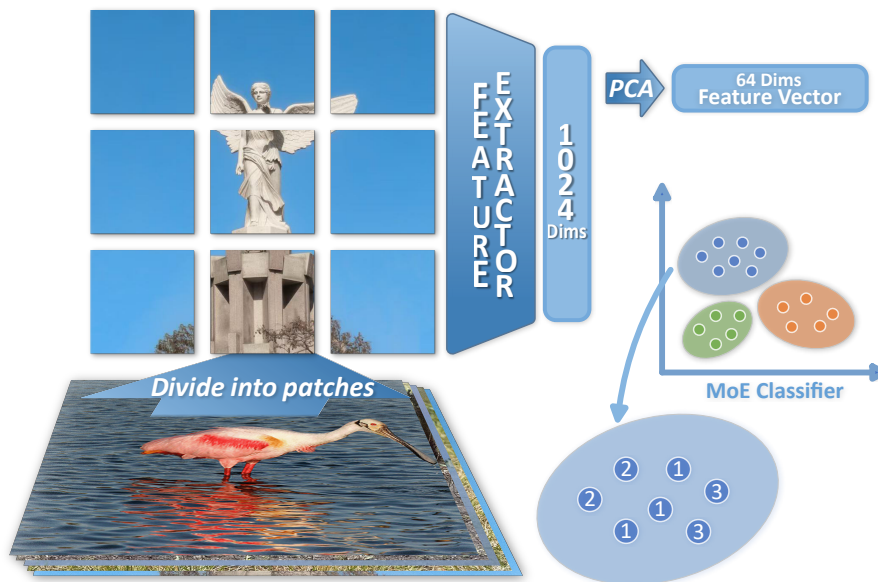


Figure 1: Overview of our SemiOccam network. The network consists of a feature extractor and a semi-supervised mixture of experts classifier. An example of a sub-model is shown in the ellipse at the bottom right, where the circle labeled ① represents a feature vector with a corresponding label, ② represents a pseudo-labeled feature vector, and ③ represents an unlabeled feature vector.

This approach achieves superior classification performance within the framework of mixture density estimation, significantly **overcomes the limitations of traditional methods** in terms of *training cost* and *model generalization performance*. Taking the Dino with ViT-large backbone as our feature extraction model, we validated the proposed semi-supervised gaussian mixture model (SGMM) method on various datasets, results show that our method **achieves state-of-the-art performance within minutes on a single Tesla T4 accelerator** and exhibits good stability and robustness, enabling **fast iteration** and potential for **edge deployment**.

It is worth mentioning that we have revealed a serious problem that has been overlooked by existing semi-supervised learning research: there are **7,500+ duplicate samples between the training samples and the testing samples in STL-10**, which is undoubtedly a serious data leakage problem when directly used for semi-supervised learning tasks. To address this, we **release the deduplicated CleanSTL-10 dataset** for fair and reliable evaluation.

Our **main contributions** can be summarized as follows:

We **introduce** the powerful ViT as a feature extractor into the classical yet often underappreciated MoE classifier for image recognition tasks.

We **propose** a unified framework that effectively exploits unlabeled data by seamlessly integrating deep representation extraction and semi-supervised learning.

We **reveal** the longstanding, yet overlooked issue of training set and test set contamination in the STL-10 dataset, which has not been addressed in other works.

We **release** the deduplicated CleanSTL-10 dataset to promote fair and reliable future research.

The **remainder of this paper** is organized as follows: Section 2 reviews related works; Section 3 introduces our SemiOccam network; Section 4 demonstrates and analyzes experimental results, including both classification performance and training cost; Section 5 discusses the significance and limitations of the research findings and outlines future research directions.

2 RELATED WORKS

2.1 SEMI-SUPERVISED LEARNING AND GAUSSIAN MIXTURE MODELS

Semi-Supervised Learning has been widely applied in tasks such as image classification and speech recognition in recent years, especially in scenarios where labeled data is scarce. Early SSL methods mainly relied on generating pseudo-labels and consistency regularization.

Pseudo-Labeling is one of the classic methods in SSL, with the core idea of using an existing model to predict unlabeled data [37] and adding its predicted labels to the training set as pseudo-labels. Representative works include [12] and [39], which iteratively enhance the labeled dataset through self-training. Although pseudo-labeling methods can effectively improve model performance, they are often affected by the quality of pseudo-labels and can easily lead to model overfitting. The study by [16] explores the issue of overconfidence caused by pseudo-labels in semi-supervised learning, analyzes the source of calibration errors, and aims to improve the reliability of the model by evaluating and potentially improving methods.

Consistency Regularization methods improve the generalization ability of models by forcing them to maintain consistency on unlabeled data. The Virtual Adversarial Training method proposed by [17] enhances the robustness of the model by perturbing the input data and maintaining the stability of the prediction results. The Mean Teacher method proposed by [30] also further improves model performance by using the consistency between the predictions of the teacher model and the output of the student model. Although these methods have achieved good results in many tasks, they often rely on complex training strategies and architectural designs, and their generalization ability across different datasets still needs to be improved.

Semi-Supervised Gaussian Mixture Model is the basic probabilistic framework of our method. It combines GMM with unlabeled data and proposes a learning method that simultaneously considers both labeled and unlabeled data by maximizing the joint log-likelihood function. Our method is inspired by the classifier structure and learning algorithm proposed by Miller & Uyar, which effec-

tively leverages unlabeled data to improve performance. In addition, many impressive works, such as [42], have extended GMM by incorporating deep autoencoders for tasks like anomaly detection.

Most related to ours is the model of [40], which also uses ViT for image embedding and then applies GMM for classification. This model is very similar to SemiOccam, but it addresses the generalized category discovery problem from [31], aiming to discover new categories, whereas our work goes further to demonstrate that combining deep learning with GMM can outperform state-of-the-art methods, especially in scenarios with extremely limited labeled data, yielding significant advantages.

2.2 DEEP NEURAL NETWORKS AND VISUAL TRANSFORMERS

Deep Neural Networks have made significant progress in various supervised learning tasks in recent years. The breakthrough achieved by AlexNet, proposed by [11], in image classification tasks laid the foundation for the development of deep learning. To improve the generalization ability of Deep Neural Networks (DNN), many methods have been proposed to address overfitting issues, such as Dropout by [28] and Batch Normalization by [9]. The Residual Network (ResNet) proposed by [7] effectively solved the gradient vanishing problem in deep network training by introducing residual connections, making it possible to train deeper networks. Subsequently, DLA by [38] introduced a dynamic hierarchical attention mechanism on top of ResNet, further optimizing layer-wise interaction and feature fusion.

Visual Transformers are image classification models based on the Transformer architecture that capture global information in images through self-attention mechanisms. [5] proposed dividing images into fixed-size patches and applying self-attention mechanisms. In this way, ViT demonstrates strong performance in image classification tasks, especially on large-scale datasets, exhibiting higher generalization ability compared to traditional convolution neural network (CNN) architectures. The success of ViT has inspired many researchers to try applying it to self-supervised learning. The DINO method proposed by [1] learns useful feature representations through self-supervised pre-training of ViT models. These representations can be fine-tuned on a small amount of labeled data to achieve high classification accuracy.

Similar to our work, these two methods integrate ViT with machine learning techniques. [32] combines CNN and ViT to better capture both local and global features, while [25] enhances hyperspectral image classification by refining the attention mechanism and adding an auxiliary branch. Both approaches optimize the ViT architecture to improve performance and efficiency in specific tasks.

2.3 SELF-SUPERVISED LEARNING AND DATA LEAKAGE ISSUES

Self-Supervised Learning is an unsupervised learning approach that automatically learns feature representations through pretext tasks (e.g., image jigsaw puzzles, predicting future frames). The CLIP model proposed by [23] achieves strong image understanding capabilities through self-supervised learning of image-text contrast, making its performance on unlabeled data very prominent.

In addition, methods like SimCLR from [3] and MoCo from [8] train neural networks through contrastive learning, enabling them to learn discriminative features without labeled data. These methods provide higher quality representations for feature extractors, thereby improving the performance of downstream tasks (such as classification, face recognition, etc.).

Data leakage issue has always been a potential challenge in machine learning. Off-topic images, near-duplicate images, and labeling errors in benchmark datasets can lead to inaccurate estimations of model performance. Handling and removing duplicate samples has become an issue that cannot be ignored in semi-supervised learning. Therefore, Gröger et al.'s work re-examines the task of data cleaning and formalizes it as a ranking problem.

3 METHOD

We assume that the entire dataset $\mathcal{X} = \{\mathbf{x}_i \in \mathbb{R}^{H \times W \times C}, i = 1, \dots, N\}$ consists of a labeled dataset $\mathcal{X}_l = \{(\mathbf{x}_1, c_1), \dots, (\mathbf{x}_{N_l}, c_{N_l})\}$ and an unlabeled dataset $\mathcal{X}_u = \{\mathbf{x}_{N_l+1}, \dots, \mathbf{x}_N\}$. Here, the number of labeled data N_l is much smaller than the total data amount N ($N_l \ll N$).

Our method is as follows:

3.1 POWERFUL FEATURE EXTRACTOR

For each input image $\mathbf{x}_i \in \mathcal{X}$, where $\mathbf{x}_i \in \mathbb{R}^{H \times W \times C}$, we divide it into a sequence of fixed-size $P \times P$ patches. Let $N_p = \frac{HW}{P^2}$ denote the number of patches per image. Each patch $\mathbf{p}_k^{(i)} \in \mathbb{R}^{P^2 C}$ (where $k = 1, \dots, N_p$) is flattened into a vector. Then, through a linear transformation, each patch vector $\mathbf{p}_k^{(i)}$ is mapped to a D -dimensional vector $\mathbf{z}_k^{(i)} \in \mathbb{R}^D$, expressed as:

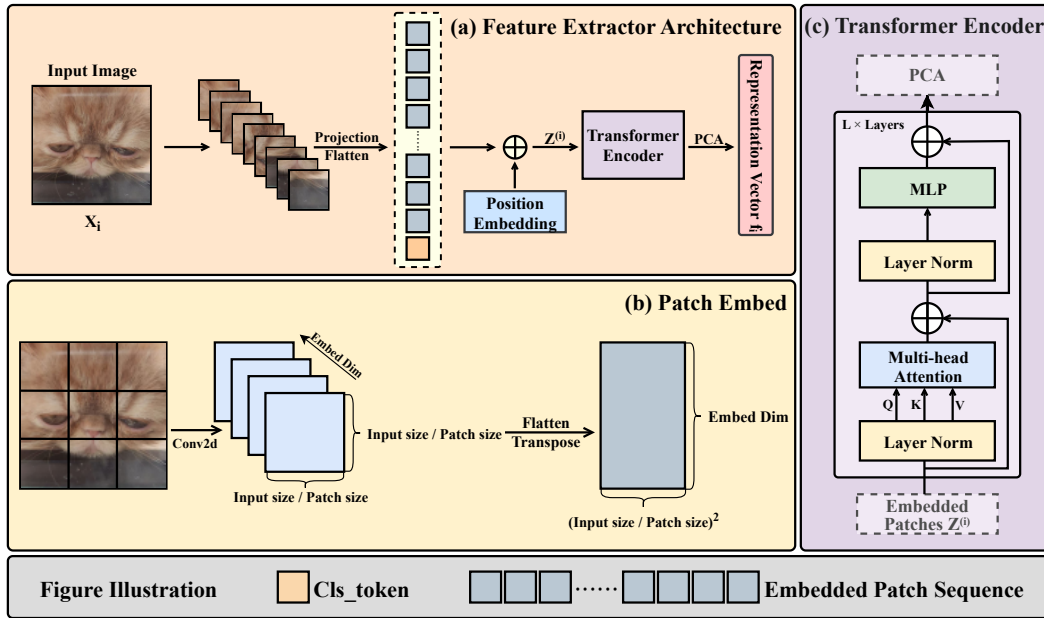


Figure 2: Feature Extraction Architecture. This diagram illustrates the ViT architecture specifically configured as a feature extractor. Input images are processed through patch embedding and a Transformer Encoder, yielding high-dimensional feature vectors for downstream tasks.

$$\mathbf{z}_k^{(i)} = \mathbf{W}\mathbf{p}_k^{(i)} + \mathbf{b} \quad (1)$$

where $\mathbf{W} \in \mathbb{R}^{D \times P^2 C}$ and $\mathbf{b} \in \mathbb{R}^D$ are learnable parameters. A learnable positional embedding $\mathbf{e}_k \in \mathbb{R}^D$ is added to each patch vector $\mathbf{z}_k^{(i)}$ to retain the positional information of the image patches, yielding $\mathbf{z}_k^{\prime(i)} = \mathbf{z}_k^{(i)} + \mathbf{e}_k$. This results in the image patch sequence $\mathbf{Z}^{(i)} = \{\mathbf{z}_1^{\prime(i)}, \mathbf{z}_2^{\prime(i)}, \dots, \mathbf{z}_{N_p}^{\prime(i)}\}$.

Subsequently, the image patch sequence $\mathbf{Z}^{(i)}$ is input into a Transformer encoder. The encoder utilizes the self-attention mechanism, which is defined as:

$$\text{Attention}(\mathbf{Q}, \mathbf{K}, \mathbf{V}) = \text{softmax}\left(\frac{\mathbf{Q}\mathbf{K}^T}{\sqrt{D}}\right)\mathbf{V} \quad (2)$$

where $\mathbf{Q} = \mathbf{Z}^{(i)}\mathbf{W}_Q$, $\mathbf{K} = \mathbf{Z}^{(i)}\mathbf{W}_K$, and $\mathbf{V} = \mathbf{Z}^{(i)}\mathbf{W}_V$. Through multiple layers of Transformer encoding and Principal Component Analysis (PCA) dimensionality reduction, we finally

obtain high-quality image feature vectors $\mathbf{f}_i \in \mathbb{R}^d$ where $d < D$. The overall feature extraction pipeline is illustrated in Figure 2.

3.2 SEMI-SUPERVISED MIXTURE OF EXPERTS CLASSIFIER

Each feature vector $\mathbf{f}_i \in \mathbb{R}^d$ is obtained from the feature extractor. Each labeled sample (\mathbf{f}_i, c_i) is associated with a class label c_i belonging to the label set $\mathcal{L} = \{1, 2, \dots, K\}$, where $K = \max\{c_1, \dots, c_{N_i}\}$ represents the total number of classes.

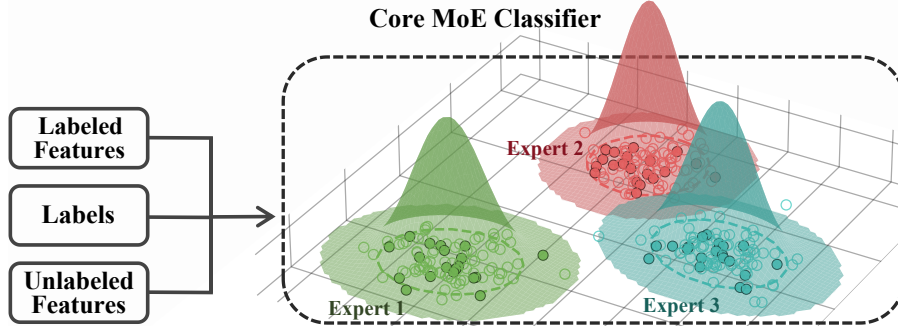


Figure 3: Illustration of our Classifier. The figure visualizes a model with three gaussian components. The solid spheres represent labeled features, while the hollow spheres denote unlabeled features.

To exploit both labeled and unlabeled data, we formulate a semi-supervised maximum likelihood estimation objective. The overall objective is:

$$\mathcal{L}(\Theta) = \mathcal{L}_1(\Theta) + \lambda \mathcal{L}_2(\Theta) \quad (3)$$

where \mathcal{L}_1 corresponds to the supervised loss, \mathcal{L}_2 to the unsupervised loss, and λ balances the two terms. In our implementation, we set $\lambda = 1$ for simplicity.

Specifically,

$$\mathcal{L}_1(\Theta) = \sum_{\mathbf{f}_i \in \mathcal{F}_l} \log p_{\Theta}(\mathbf{f}_i, c_i), \quad \mathcal{L}_2(\Theta) = \sum_{\mathbf{f}_i \in \mathcal{F}_u} \log p_{\Theta}(\mathbf{f}_i) \quad (4)$$

The joint likelihood of all samples can thus be written as:

$$\mathcal{L}(\Theta) = \underbrace{\sum_{\mathbf{f}_i \in \mathcal{F}_l} \log \sum_{l=1}^L \pi_l p(\mathbf{f}_i | \theta_l) P(c_i | l)}_{\text{labeled data likelihood}} + \underbrace{\sum_{\mathbf{f}_i \in \mathcal{F}_u} \log \sum_{l=1}^L \pi_l p(\mathbf{f}_i | \theta_l)}_{\text{unlabeled data likelihood}} \quad (5)$$

where $\Theta = \{\pi_l, \boldsymbol{\mu}_l, \boldsymbol{\Sigma}_l, P(c|l)\}_{l=1 \dots L, c=1 \dots K}$ is the set of model parameters with $\sum_{l=1}^L \pi_l = 1$, π_l represents the mixing coefficient of the l -th gaussian component, $p(\mathbf{f}_i | \theta_l)$ is the probability density function of the l -th gaussian component with parameters $\theta_l = \{\boldsymbol{\mu}_l, \boldsymbol{\Sigma}_l\}$, and $P(c_i | l)$ represents the conditional probability that a feature belongs to class c_i given gaussian component l .

The EM algorithm updates parameters as follows:

$$\gamma_{il}^{(t)} = \frac{\pi_l^{(t)} p(\mathbf{f}_i | \theta_l^{(t)})}{\sum_{j=1}^L \pi_j^{(t)} p(\mathbf{f}_i | \theta_j^{(t)})} \quad \forall \mathbf{f}_i \in \mathcal{F}_u \quad (6)$$

$$\gamma_{il|c_i}^{(t)} = \frac{\pi_l^{(t)} p(\mathbf{f}_i|\theta_l^{(t)}) P(c_i|l)^{(t)}}{\sum_{j=1}^L \pi_j^{(t)} p(\mathbf{f}_i|\theta_j^{(t)}) P(c_i|j)^{(t)}} \quad \forall \mathbf{f}_i \in \mathcal{F}_l \quad (7)$$

$$\boldsymbol{\mu}_l^{(t+1)} = \frac{\sum_{\mathbf{f}_i \in \mathcal{F}_l} \mathbf{f}_i \gamma_{il|c_i}^{(t)} + \sum_{\mathbf{f}_i \in \mathcal{F}_u} \mathbf{f}_i \gamma_{il}^{(t)}}{\sum_{\mathbf{f}_i \in \mathcal{F}_l} \gamma_{il|c_i}^{(t)} + \sum_{\mathbf{f}_i \in \mathcal{F}_u} \gamma_{il}^{(t)}} \quad (8)$$

$$\boldsymbol{\Sigma}_l^{(t+1)} = \frac{\sum_{\mathbf{f}_i \in \mathcal{F}_l} M_{il}^{(t)} \gamma_{il|c_i}^{(t)} + \sum_{\mathbf{f}_i \in \mathcal{F}_u} M_{il}^{(t)} \gamma_{il}^{(t)}}{\sum_{\mathbf{f}_i \in \mathcal{F}_l} \gamma_{il|c_i}^{(t)} + \sum_{\mathbf{f}_i \in \mathcal{F}_u} \gamma_{il}^{(t)}} \quad (9)$$

where $M_{il}^{(t)} = (\mathbf{f}_i - \boldsymbol{\mu}_l^{(t)})(\mathbf{f}_i - \boldsymbol{\mu}_l^{(t)})^\top$.

$$\pi_l^{(t+1)} = \frac{1}{N} \left(\sum_{\mathbf{f}_i \in \mathcal{F}_l} \gamma_{il|c_i}^{(t)} + \sum_{\mathbf{f}_i \in \mathcal{F}_u} \gamma_{il}^{(t)} \right) \quad (10)$$

$$P(k|l)^{(t+1)} = \frac{\sum_{\mathbf{f}_i \in \mathcal{F}_l, c_i=k} \gamma_{il|c_i}^{(t)}}{\sum_{\mathbf{f}_i \in \mathcal{F}_l} \gamma_{il|c_i}^{(t)}} \quad (11)$$

The model learns its optimal parameters, Θ , by iterating between the Expectation and Maximization until the algorithm converges. Figure 3 offers a visual illustration of the final learned state, presenting a classifier made up of three gaussian components.

3.3 PSEUDO-LABELING MECHANISM

To effectively leverage information from the unlabeled dataset \mathcal{X}_u , we introduce a pseudo-labeling mechanism based on the *component-class association probabilities*. Unlike traditional iterative methods, our pseudo-label generation is performed in a single calculation after the initial SGMM training reaches convergence, reducing computational cost and mitigating error accumulation risks.

For unlabeled features $\mathbf{f}_i \in \mathcal{F}_u$, we compute class probabilities through gaussian component responsibilities:

$$p_i^{(k)} = \sum_{l=1}^L P(k|l)^{(t)} \gamma_{il}^{(t)}, \quad \xi_i = \max_{1 \leq k \leq K} p_i^{(k)} \quad (12)$$

where $P(k|l)$ represents the class probability conditioned on component l , and $\gamma_{il}^{(t)}$ is the responsibility from Equation 6.

We construct class-specific candidate sets with confidence thresholding sorted by ξ_i descending:

$$\mathcal{C}_k = \left\{ \mathbf{f}_i \mid \arg \max_k p_i^{(k)} = k, \xi_i > \tau, \tau \in (0, 1) \right\} \quad (13)$$

To prevent class imbalance, we adopt proportional sampling:

$$n^{\text{final}} = \min_{1 \leq k \leq K} [\alpha |\mathcal{C}_k|] \quad (\alpha \in (0, 1)) \quad (14)$$

The pseudo-labeled set is then constructed as:

$$\mathcal{D}_p = \{(\mathbf{f}_i, k) \mid k = 1, \dots, K, \mathbf{f}_i \in \mathcal{C}_k[1 : n^{\text{final}}]\} \quad (15)$$

Finally, combine the pseudo-labeled data \mathcal{D}_p with the labeled features \mathcal{F}_l and use the EM algorithm for iterative. We use Kmeans++ to initialize the parameters first, during the training process, log-likelihood value calculated using Equation 5 increases steadily. We show the procedure of our method in Algorithm 1.

Algorithm 1 SemiOccam Network

Require: Labeled data \mathcal{X}_l , Unlabeled data \mathcal{X}_u , Pre-trained ViT, SGMM components L , Confidence threshold τ , Sampling ratio α

Ensure: Trained SGMM parameters Θ

- 1: Extract features $\mathcal{F}_l \leftarrow \{\text{ViT}(\mathbf{x}_i) | (\mathbf{x}_i, c_i) \in \mathcal{X}_l\}$ and $\mathcal{F}_u \leftarrow \{\text{ViT}(\mathbf{x}_i) | \mathbf{x}_i \in \mathcal{X}_u\}$
 - 2: PCA \mathcal{F}_l and \mathcal{F}_u into \mathbb{R}^d
 - 3: L centers cluster $\mathcal{F}_l \cup \mathcal{F}_u$ with K-means++
 - 4: Initialize $\{\pi_l, \mu_l, \Sigma_l\}$ from cluster results
 - 5: **for** $t = 1$ to T_1 **do**
 - 6: EM algorithm: Initial iterative via (6-11)
 - 7: **end for**
 - 8: Construct \mathcal{D}_p using (13-15) with τ and α
 - 9: Augment labeled set: $\mathcal{F}_l \leftarrow \mathcal{F}_l \cup \mathcal{D}_p$
 - 10: **for** $t = 1$ to T_2 **do**
 - 11: EM algorithm: Final iterative via (6-11)
 - 12: **end for**
 - 13: **return** Θ
-

4 EXPERIMENTS

4.1 STANDARD SGMM PERFORMANCE ANALYSIS

The performance of the SGMM is influenced by several factors. This section will delve into the impact of the number of labels, feature dimensions, and the number of gaussian components on the model’s behavior.

SGMM’s core of its labeling efficiency lies in using unlabeled data to assist the model in learning the data distribution. Theoretically, as the number of labeled samples increases, the model can more accurately estimate the conditional probability of categories $P(k|l)$, thereby improving discrimination ability. When the labeled samples reach a certain scale, the marginal benefit of the additional information provided by unlabeled data diminishes, and the performance improvement curve tends to flatten. Therefore, SGMM’s advantage is that it can quickly improve performance with very few labels and demonstrate high efficiency in applications with limited labeling resources.

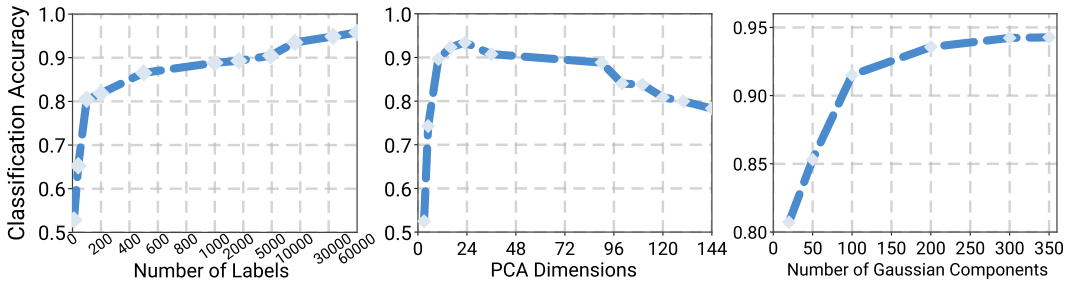


Figure 4: Relationship between number of labels/PCA dimensions/number of gaussian components and performance on the MNIST dataset. The first figure shows a steady improvement in accuracy with an increase in labels. The second figure shows the trend of SGMM accuracy with PCA dimensions, while the right figure shows the trend of accuracy with the number of gaussian submodels.

When dealing with high-dimensional data, the feature dimension is crucial to the performance and computational efficiency of SGMM. High-dimensional feature spaces can lead to the “curse of dimensionality”, increasing the complexity of model training and the risk of overfitting, while also

consuming excessive computational resources. Reducing feature dimensions through dimensionality reduction techniques such as PCA can retain discriminative feature information while removing redundant dimensions, alleviating these problems to some extent. However, excessive dimensionality reduction can lead to the loss of key feature information. Therefore, the feature dimension should be reduced as much as possible while ensuring model performance.

Gaussian Mixture Models use multiple gaussian components to fit complex data distributions, and the number of components directly affects the model’s complexity and fitting ability. When the number of components is small, the model may not be able to fully capture the fine-grained structure of the data distribution, leading to underfitting. When the number of components is too large, the model complexity increases, which can easily lead to overfitting of the training data, reducing generalization ability and increasing computational costs. Therefore, the optimal number of gaussian components should match the intrinsic class structure and complexity of the dataset.

In summary, labeling efficiency reflects the core advantage of semi-supervised learning. Feature dimension efficiency emphasizes the role of dimensionality reduction in improving model efficiency and generalization ability. The number of gaussian components reflects the trade-off between model complexity and data fitting ability. Understanding the impact of these factors on SGMM performance helps to adjust model parameters according to specific tasks in practical applications.

4.2 MORE POWERFUL FEATURE EXTRACTORS

To further analyze the performance of the SGMM, we experimented on the CIFAR-10 dataset using different feature extractors: PCA, DNNs (ResNet101, DLA169), and ViT-Base/Large backbone DINO pre-trained models. Figure 5 shows that with DNNs and ViTs, increasing the number of gaussian components leads to a decrease in classification accuracy, which contrasts with the performance trend observed when using PCA.

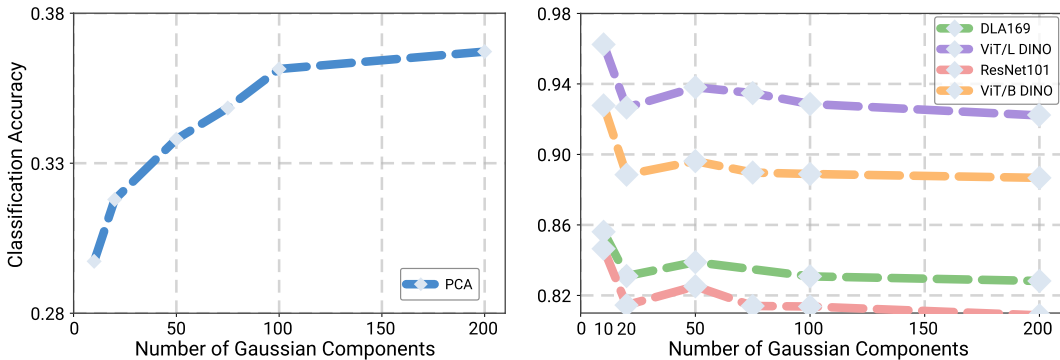


Figure 5: Performance trends. The left figure shows the accuracy trend of SGMM on the CIFAR-10 dataset processed with PCA, while the right figure shows the accuracy trend with the number of gaussian submodels when using DNNs and ViTs.

Next, we performed t-SNE visualization on the features extracted by the three methods. In Figure 6, we present the t-SNE visualization results of feature representations obtained using different feature extraction methods on the CIFAR-10 dataset. It can be clearly seen from the figure that the feature points extracted by PCA exhibit a highly mixed state in the t-SNE space, and it is difficult to distinguish between samples from different categories. This indicates that the feature representation after PCA dimensionality reduction lacks sufficient discriminative power. In contrast, the feature points extracted using deep neural networks exhibit a certain clustering trend in the t-SNE space, but there is still some overlap between the boundaries of different categories. The feature points extracted using Visual Transformer form a relatively clear cluster structure in the t-SNE space, which indicates that the feature representation extracted by ViT has stronger separability and can better capture the intrinsic structure of the data, providing a more favorable feature basis for subsequent classification tasks.

PCA has limited feature discrimination ability, so it needs more gaussian sub-models to model complex intra-class variations. At this time, increasing the number of gaussian components helps

to approximate the true distribution; while the features extracted by DNN/ViT are close to a single gaussian for each category, increasing the number of components will cause the model complexity to exceed the actual needs. These analyses are consistent with the experimental results in Figure 5.

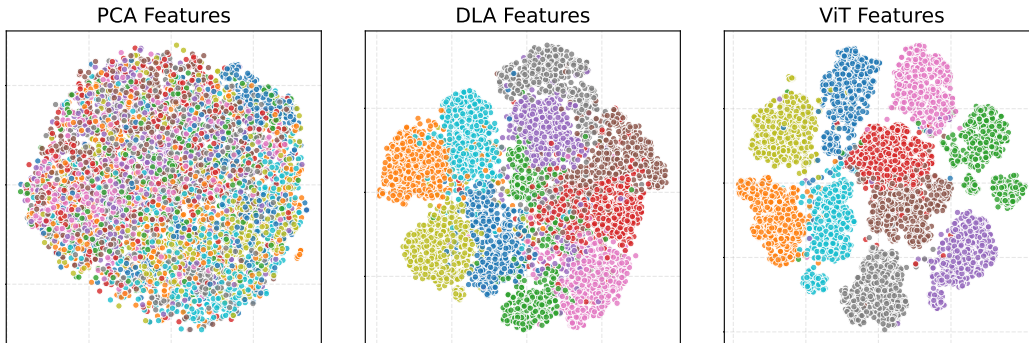


Figure 6: t-SNE Visualization. t-SNE visualization results of different feature extraction methods on the CIFAR-10 dataset.

We analyzed high-confidence samples from two gaussian components of the same bird category. Observing the original images in Figure 7, we found that these two gaussian components exhibit different feature preferences: one component tends to give high confidence to samples of ostriches (long-necked birds), while the other component prefers plump, neckless birds.

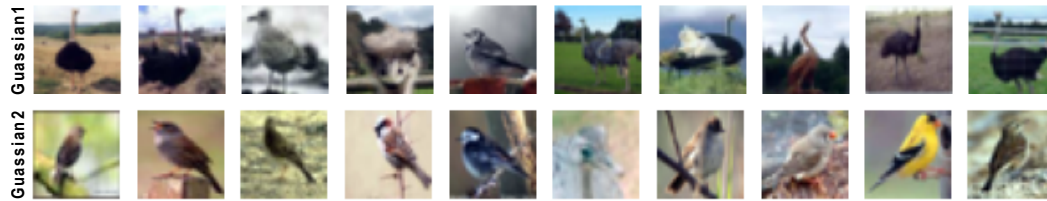


Figure 7: Comparison raw images. Visualization of high-confidence samples from two gaussian components of the bird category on the CIFAR-10 dataset.

We compare the heatmaps of DNN and ViT on several randomly selected images from the internet, each containing two animals simultaneously. The heatmaps are generated using the Grad-CAM method, which visualizes the importance of each pixel in the image for the classification result. As shown in Figure 8, the heatmaps of DNN and ViT differ significantly. While DNN focuses primarily on one animal, ViT attends to both animals in the image, demonstrating its ability to capture global context more effectively. This comparison highlights the differences in how these models prioritize regions of the image during classification. Through experimental results and visualization analysis, we found that DNN and ViT can better capture the distribution characteristics of data compared to the traditional PCA dimensionality reduction method, thereby improving the classification performance of SGMM.

4.3 STL-10 DATA CLEAN

Duplicate samples in the STL-10 dataset can potentially bias model evaluation. To address this, we deduplicated the dataset. Specifically, we used a script to compute image hashes for STL-10 dataset, then removed 7,545 samples from the train set that were found to be duplicates of samples in the test set. **We release the deduplicated CleanSTL-10 dataset** to facilitate fair and reliable research. The pseudo-code for this deduplication process is provided in Algorithm 2.

Following processing, the training set consists of 5,000 labeled samples and 90,455 unsupervised samples. This effectively addresses the problem of data leakage, thereby guaranteeing the credibility of the experimental findings.

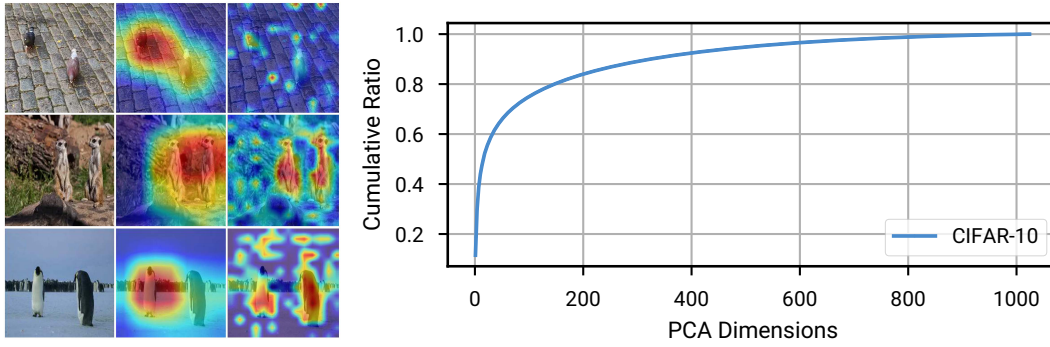


Figure 8: Visual comparison of feature attention (left) and PCA variance analysis (right).

Algorithm 2 Deduplication of Dataset

Require: Main dataset, test dataset, batch size

Ensure: Deduplicated dataset, CSV file with duplicate information

```

Build test set hash dictionary: Compute hash for each test image
2: Initialize valid_indices and duplicates as empty lists
for each batch in main dataset do
4:   for each image in batch do
      Compute hash of the image
6:     if hash exists in test set hash dictionary then
          Record duplicate sample details
8:     else
          Add current index to valid_indices
10:    end if
      end for
12: end for
if duplicates is not empty then
14:   Save duplicate details to CSV file
      end if

```

Table 1: Example pairs of training and test samples sharing the same hash value.

Train Index	Test Index	Hash
5008	2075	e777922f14273159776a089a6f44d2bbb03f23a2b618f0914ef7ca442e770396
5025	4149	d91a18f5a643aaf3569387641a6f40a92ec82a32a27a532625414dbaf48b4d25
5032	6188	eadb8e0cd40606bb3e6c58f710abb4d9769e43b43724ef764e7a74a4d179fff4
5041	4228	5c1dee15a65d67508008125e0f1085382084a860e491c10f0f6c15d7c7d06a36
5045	6029	f4197466cd0d97da2a2b079bc7458d7af8d1c89a7178d30d14668364037d165a
5062	4980	82a4e1da419ea969f5bc07f9664e8974dee8c8161334d0ad9abc89f9545e8f41
5071	7166	b445c22c7f8505e1ac09d6efa5b756daac42da5ae70acd8d672b9c164c4c8bbc
5072	7091	9fb660ef9603189ca18787bcf60966bc8cb07f6ad121eeb3602cb543a5123830
5073	2803	7e3753d43ea8769a2818d947feca2beb84cf5e3cb090d5b31c820e6f6f4f0d8a
5092	6820	c360dd72cb9f9056302cafbcb2f5ccfe9de66fddac0b8ed4d91ce93996dd98503
5108	5761	03a02e10956c65799a5f5d082d61cbaf1de414773c7c025da8fbfc5553c6fdf0
5121	2143	8e98699fcf6ec4e0b8765866248e7702c2f26f9fe2d1f469eeb0f51f54bb5afb
5129	1287	363360e93d8997c1138d1e4a0fde65b7b08befd496b450df72989aac5e5b4eddb
5139	3879	b2fa77caa967437f1a85c6071b2345d420da69780036d44f761591ad6d213ff6
5143	4701	29b8233f6d9a24cfbbdd83f23c838d59b1a113ada232c0991bd63e1fa97c533e
5165	6844	46f4be3edd44d770964fb27f6777e77f5a93d1623921c9d630f9454908f9e2ac
5169	4665	ee864c70c6d01868bcde6eb61261c33057f39efbe9197a7590aed629a4215bae
5172	461	aa81e6c7a9a3c597b331abd352271f91eb4f1129b41cfff164b35371c41a8217
5188	2893	0da766b7fe175d6cb8328437019e4fa2d87f4878cdb09e9b2d001fe6374a100e
5191	4131	b909207b8b5822d2a2197ab4563fc32def9b9d04934285928a0ad6f08d1de9f4
5197	6931	013a41f75629ce371fbbec3f9a845aa5ec3e615819a4e4ae67b3dbe0d70ece0d
5214	991	9a3201824495feabca12e1ef2339c410ff1f30c412ff35d85743bcd16f6bcabc
5226	196	7309f100d4dc411520175d905e2cdebdd3ace6422ec0310efb61f7a93052402b

We present an example table of training and test sample indices with duplicate hash values in Table 1. The full list can be found in our project repository.

4.4 EXPERIMENT SETUP

Datasets. We report results on the Cifar-10/100 and CleanSTL-10 datasets. CIFAR-10 contains 10 classes with 6,000 32x32 color images per class, totaling 60,000 images, of which 50,000 are for training and 10,000 for testing. CIFAR-100 is similar to CIFAR-10 but contains 100 classes with 600 images per class, of which 500 are for training and 100 for testing. STL-10 is an image classification dataset designed for self-supervised and semi-supervised learning, containing 10 classes with 5,000 labeled training samples and 100,000 unlabeled images, each at a resolution of 96x96 pixels. We created CleanSTL-10 by carefully removing duplicates and overlaps between training and test sets, as detailed in Section 4.3. After this deduplication, CleanSTL-10 contains 90,455 training images and 8,000 testing images, ensuring more reliable and fair evaluation.

Implementation details. We use the DINO pre-trained model with a ViT-Large backbone to extract feature representations. For dimensionality reduction, PCA is applied with dimensions selected based on explained variance, typically preserving over 60% of the total variance (see Fig. 8). On the CIFAR-10 and CIFAR-100 datasets, we set the number of gaussian components to 10 and 100, respectively, and the PCA dimension to 60. For CleanSTL-10, which contains more than 10 categories in its training set, we set the number of gaussian components to 15 for improved robustness, the PCA dimension to 45, and the convergence threshold (Tol) to 10^1 . Classification performance is evaluated using accuracy. All experiments are conducted on a single NVIDIA Tesla T4 accelerator with 15 GB of memory.

4.5 COMPARISON WITH STATE-OF-THE-ART METHODS

Results on CIFAR-10. We show the benchmark results on CIFAR-10 in Table 2. Our method achieves competitive performance compared with state-of-the-art methods, including FlexMatch [39], SequenceMatch [19] and EPASS [20]. It can be clearly seen that our method consistently outperforms other methods under all settings.

Table 2: Benchmark results on CIFAR-10.

Algorithms	Error Rate (40 labels)	Error Rate (250 labels)	Error Rate (4000 labels)
Dash (2021)	9.29 ± 3.28	5.16 ± 0.23	4.36 ± 0.11
MPL (2021)	6.62 ± 0.91	5.76 ± 0.24	4.36 ± 0.11
FlexMatch (2021)	4.97 ± 0.06	4.98 ± 0.09	4.19 ± 0.01
CoMatch (2021)	6.51 ± 1.18	5.35 ± 0.14	4.27 ± 0.12
SimMatch (2022)	5.38 ± 0.01	5.36 ± 0.08	4.41 ± 0.07
AdaMatch (2022)	5.09 ± 0.21	5.13 ± 0.05	4.36 ± 0.05
FreeMatch (2023)	4.90 ± 0.12	4.88 ± 0.09	4.16 ± 0.06
SoftMatch (2023)	5.11 ± 0.14	4.96 ± 0.09	4.27 ± 0.05
SequenceMatch (2024)	4.80 ± 0.01	4.75 ± 0.05	4.15 ± 0.01
EPASS (2024)	5.55 ± 0.21	5.31 ± 0.13	4.23 ± 0.05
SemiOccam (Ours)	3.51 ± 0.12	3.47 ± 0.17	3.45 ± 0.16

Results on CleanSTL-10. In Table 3, we present the performance on CleanSTL-10. Our method achieves state-of-the-art performance, outperforming other methods by a large margin. Our method achieves the best performance in all three settings, demonstrating the effectiveness of our proposed method. Compared to SequenceMatch in 2024, our SemiOccam achieves +10.88%, +8.35%, and +1.41% on 40-label, 250-label, and 1000-label settings, respectively.

Table 3: Benchmark results on CleanSTL-10.

Algorithms	Error Rate (40 labels)	Error Rate (250 labels)	Error Rate (1000 labels)
Dash (2021)	42.00 ± 4.94	10.50 ± 1.37	6.30 ± 0.49
MPL (2021)	35.97 ± 4.14	9.90 ± 0.96	6.66 ± 0.00
FlexMatch (2021)	29.12 ± 5.04	9.85 ± 1.35	6.08 ± 0.34
CoMatch (2021)	13.74 ± 4.20	7.63 ± 0.94	5.71 ± 0.08
SimMatch (2022)	16.98 ± 4.24	8.27 ± 0.40	5.74 ± 0.31
AdaMatch (2022)	19.95 ± 5.17	8.59 ± 0.43	6.01 ± 0.02
FreeMatch (2023)	28.50 ± 5.41	9.29 ± 1.24	5.81 ± 0.32
SoftMatch (2023)	22.23 ± 3.82	9.18 ± 0.63	5.79 ± 0.15
SequenceMatch (2024)	15.45 ± 1.40	12.78 ± 0.76	5.56 ± 0.35
EPASS (2024)	9.15 ± 3.25	6.27 ± 0.03	5.40 ± 0.12
SemiOccam (Ours)	4.57 ± 0.24	4.43 ± 0.08	4.15 ± 0.07

Results on CIFAR-100. In Table 4, we compare the performance of SemiOccam with state-of-the-art methods on CIFAR-100 dataset. Our method outperforms other methods in the 400 labels and 2,500 labels setting, and achieves comparable 10,000 labels settings.

Table 4: Benchmark results on CIFAR-100.

Algorithms	Error Rate (400 labels)	Error Rate (2500 labels)	Error Rate (10000 labels)
Dash (2021)	44.82 ± 0.96	27.15 ± 0.22	21.88 ± 0.07
MPL (2021)	46.26 ± 1.84	27.71 ± 0.19	21.74 ± 0.09
FlexMatch (2021)	39.94 ± 1.62	26.49 ± 0.20	21.90 ± 0.15
CoMatch (2021)	53.41 ± 2.36	29.78 ± 0.11	22.11 ± 0.22
SimMatch (2022)	39.32 ± 0.72	26.21 ± 0.37	21.50 ± 0.11
AdaMatch (2022)	38.08 ± 1.35	26.66 ± 0.33	21.99 ± 0.15
FreeMatch (2023)	39.52 ± 0.01	26.22 ± 0.08	21.81 ± 0.17
SoftMatch (2023)	37.60 ± 0.24	26.39 ± 0.38	21.86 ± 0.16
SequenceMatch (2024)	37.86 ± 1.07	25.99 ± 0.22	20.10 ± 0.04
EPASS (2024)	38.88 ± 0.24	25.68 ± 0.33	21.32 ± 0.14
SemiOccam (Ours)	26.59 ± 1.02	22.19 ± 0.81	21.21 ± 0.26

4.6 ABLATION STUDY

We conduct comprehensive ablation experiments to evaluate the effectiveness of different components in our SemiOccam framework. Table 5 summarizes the classification error rates across three datasets under various settings.

4.6.1 EFFECTIVENESS OF SGMM VS. SOFTMAX CLASSIFIER

To evaluate the benefit of using the SGMM component, we replace it with the standard ViT classification head based on a softmax layer and train both models under limited-label settings. The results in Table 5 show that SemiOccam significantly outperforms the softmax-based head, especially in extremely low-label regimes.

ViT Classification Head for Semi-Supervised Learning. We define the original ViT head as follows: Given the feature vector $\mathbf{f}_i \in \mathbb{R}^d$ extracted from the backbone, a linear projection is applied as $\mathbf{s}_i = \mathbf{W}_h \mathbf{f}_i + \mathbf{b}_h$, followed by a softmax function:

$$P(c = k | \mathbf{f}_i) = \frac{\exp(s_{i,k})}{\sum_{j=1}^K \exp(s_{i,j})}, \quad \forall k \in \{1, \dots, K\}$$

We adopt a confidence-based pseudo-labeling scheme to construct the unsupervised loss. The overall training objective combines both supervised and unsupervised loss terms:

$$\mathcal{L}_{\text{total}} = \mathcal{L}_{\text{sup}} + \lambda(t) \cdot \mathcal{L}_{\text{unsup}}, \quad \lambda(t) = \lambda_{\text{max}} \cdot \min\left(1, \frac{t}{T_{\text{ramp}}}\right)$$

4.6.2 IMPACT OF PSEUDO-LABELING

We further examine the effect of pseudo-labeling by disabling it in training. The row labeled “w/o P-L” in Table 5 shows that removing pseudo-labeling leads to degraded performance, highlighting its importance for leveraging unlabeled data effectively.

Table 5: Ablation results on CIFAR-10/100 and CleanSTL-10.

Dataset	CIFAR-10			CIFAR-100			CleanSTL-10		
	# Labels	40	250	4000	400	2500	10000	40	250
w Softmax	51.05 ± 16.69	5.40 ± 1.70	3.75 ± 0.21	57.32 ± 10.91	43.01 ± 5.89	33.70 ± 2.71	16.29 ± 2.85	4.88 ± 1.50	4.38 ± 0.40
w/o P-L	3.73 ± 0.21	3.70 ± 0.23	3.63 ± 0.19	30.56 ± 0.80	23.21 ± 0.66	21.56 ± 0.43	4.91 ± 0.12	4.81 ± 0.12	4.58 ± 0.10
SemiOccam	3.51 ± 0.12	3.47 ± 0.17	3.45 ± 0.16	26.59 ± 1.02	22.19 ± 0.81	21.21 ± 0.26	4.44 ± 0.04	4.43 ± 0.08	4.15 ± 0.07

4.7 TRAINING COST ANALYSIS

In the field of semi-supervised learning, besides model performance, training overhead is a key metric for evaluating the practicality and environmental impact of algorithms. This section will quantitatively compare the training overhead of existing benchmarks with our proposed method.

TorchSSL from Zhang et al. is a mainstream SSL evaluation protocols, typically employ training deep neural networks from scratch, leading to significant computational burdens. For example, training the FixMatch algorithm on a single **NVIDIA V100 GPU** requires “300 hours × 3 settings × 3 seeds” for the CIFAR-100 dataset; “110 hours × 3 settings × 3 seeds” for CIFAR-10; and “225 hours × 3 settings × 3 seeds” for STL-10. The total training time amounts to **5715 GPU hours** (approximately 238 GPU days). This high computational demand poses a significant experimental cost barrier for academia and resource-constrained research institutions.

USB from Wang et al. is another current mainstream SSL evaluation protocol. It reports that training the FixMatch algorithm on a single **NVIDIA V100 GPU** incurs an overhead of “11 hours × 2 settings × 3 seeds” for the CIFAR-100 dataset, and “18 hours × 2 settings × 3 seeds” for the STL-10 dataset. Across these two datasets, a total of **174 GPU hours are required**.

Our proposed method utilizes a pre-trained ViT as a feature extractor. After this feature extraction step is completed, our core classifier training process can typically be completed in **less than ten minutes** on a **single free Tesla T4 accelerator** on the Google Colab platform, demonstrating high efficiency and state-of-the-art performance. This minute-level training time gives our method a significant competitive advantage in **resource-constrained practical deployments** and **rapid iteration research scenarios**. For detailed training time performance, please refer to Figure 9.

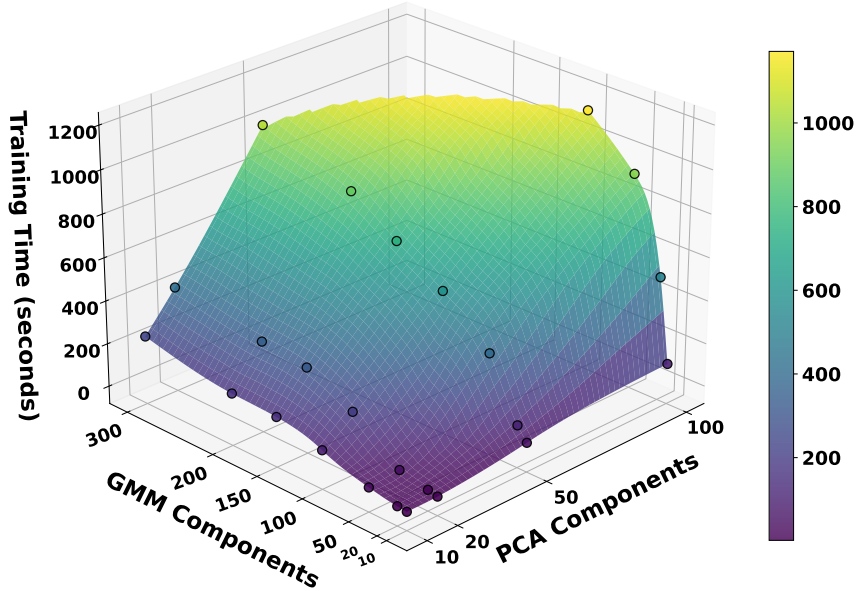


Figure 9: Our Core Training Time Analysis. This surface plot illustrates the training time (in seconds) of the SGMM classifier under varying numbers of GMM and PCA components, assuming a 60,000-sample training dataset.

5 CONCLUSIONS

We introduce high-performance feature extractors into the classical yet often underappreciated MoE classifier for image recognition tasks. Our architecture is simple and **training is highly efficient**, making it particularly **well-suited for scenarios with limited labeled data**. The proposed unified modeling strategy performs surprisingly well when trained with very few labeled samples and large-scale unlabeled data. In our study, we also **identify a long-overlooked data leakage issue** in the STL-10 dataset and **release the deduplicated CleanSTL-10 dataset** to ensure fair and reliable evaluation in semi-supervised learning. Extensive experiments show that SemiOccam **achieves new performance breakthroughs** on benchmarks such as CleanSTL-10 and CIFAR-10, maintaining over 96% classification accuracy even with only 4 labeled samples per class **in under ten minutes** on a single Tesla T4 accelerator, compared to the hundreds of GPU hours required by existing methods.

Future development of this technology can proceed along several dimensions. **First**, constructing dynamic component adjustment mechanism based on a Bayesian framework to achieve parameter adaptivity. **Secondly**, enhancing the model’s discriminative performance when facing complex tasks such as fine-grained classification. **Most interesting**, exploring its application in other fields, such as electroencephalogram signal analysis and medical image processing, thereby broadening its application scope and verifying its transferability.

We believe these improvements will further unlock the technological benefits brought about by the fusion of probabilistic graphical models and deep learning. **Crucially**, given our method’s advantages in short training times and high efficiency, we are particularly keen to see its widespread **adoption in edge deployment scenarios and applications requiring rapid iteration**.

ACKNOWLEDGMENTS

The work is supported by the National Natural Science Foundation of China No. 62076078, Fundamental Research Funds for the Central Universities No.3072024LJ0403, and the CAAI-Huawei MindSpore Open Fund No. CAAIXSJLJJ-2020-033A.

REFERENCES

- [1] Mathilde Caron, Hugo Touvron, Ishan Misra, Hervé Jégou, Julien Mairal, Piotr Bojanowski, and Armand Joulin. Emerging properties in self-supervised vision transformers. In *Proceedings of the IEEE/CVF international conference on computer vision*, pp. 9650–9660, 2021.
- [2] Hao Chen, Ran Tao, Yue Fan, Yidong Wang, Jindong Wang, Bernt Schiele, Xing Xie, Bhiksha Raj, and Marios Savvides. Softmatch: Addressing the quantity-quality trade-off in semi-supervised learning. In *International Conference on Learning Representations (paper)*, 2023.
- [3] T Chen, S Kornblith, M Norouzi, and G Hinton. Simclr: A simple framework for contrastive learning of visual representations [c]. *International Conference on Learning Representations*, 2020.
- [4] Jeremy Chopin and Rozenn Dahyot. Performance of gaussian mixture model classifiers on embedded feature spaces, 2024.
- [5] Alexey Dosovitskiy, Lucas Beyer, Alexander Kolesnikov, Dirk Weissenborn, Xiaohua Zhai, Thomas Unterthiner, Mostafa Dehghani, Matthias Minderer, Georg Heigold, Sylvain Gelly, Jakob Uszkoreit, and Neil Houlsby. An image is worth 16x16 words: Transformers for image recognition at scale, 2021.
- [6] Fabian Gröger, Simone Lionetti, Philippe Gottfrois, Alvaro Gonzalez-Jimenez, Ludovic Amruthalingam, Matthew Groh, Alexander A Navarini, and Marc Pouly. Intrinsic self-supervision for data quality audits. In *The Thirty-eight Conference on Neural Information Processing Systems Datasets and Benchmarks Track*, 2024.

- [7] Kaiming He, Xiangyu Zhang, Shaoqing Ren, and Jian Sun. Deep residual learning for image recognition. In *Proceedings of the IEEE conference on computer vision and pattern recognition*, pp. 770–778, 2016.
- [8] Kaiming He, Haoqi Fan, Yuxin Wu, Saining Xie, and Ross Girshick. Momentum contrast for unsupervised visual representation learning. In *Proceedings of the IEEE/CVF Conference on Computer Vision and Pattern Recognition (CVPR)*, June 2020.
- [9] Sergey Ioffe and Christian Szegedy. Batch normalization: accelerating deep network training by reducing internal covariate shift. In *Proceedings of the 32nd International Conference on International Conference on Machine Learning*, pp. 448–456, 2015.
- [10] Li Jing, Pascal Vincent, Yann LeCun, and Yuandong Tian. Understanding dimensional collapse in contrastive self-supervised learning. In *10th International Conference on Learning Representations, paper 2022*, 2022.
- [11] Alex Krizhevsky, Ilya Sutskever, and Geoffrey E Hinton. Imagenet classification with deep convolutional neural networks. *Advances in neural information processing systems*, 25, 2012.
- [12] Dong-Hyun Lee et al. Pseudo-label: The simple and efficient semi-supervised learning method for deep neural networks. In *Workshop on challenges in representation learning, ICML*, volume 3, pp. 896. Atlanta, 2013.
- [13] Junnan Li, Caiming Xiong, and Steven CH Hoi. Comatch: Semi-supervised learning with contrastive graph regularization. In *Proceedings of the IEEE/CVF international conference on computer vision*, pp. 9475–9484, 2021.
- [14] Michael Majurski, Sumeet Menon, Parniyan Farvardin, and David Chapman. A method of moments embedding constraint and its application to semi-supervised learning, 2024.
- [15] David J Miller and Hasan Uyar. A Mixture of Experts Classifier with Learning Based on Both Labelled and Unlabelled Data. In *Advances in Neural Information Processing Systems*, volume 9. MIT Press, 1996. URL https://proceedings.neurips.cc/paper_files/paper/1996/hash/a58149d355f02887dfbe55ebb2b64ba3-Abstract.html.
- [16] Shambhavi Mishra, Balamurali Murugesan, Ismail Ben Ayed, Marco Pedersoli, and Jose Dolz. Do not trust what you trust: Miscalibration in semi-supervised learning, 2024.
- [17] Takeru Miyato, Shin-ichi Maeda, Masanori Koyama, and Shin Ishii. Virtual adversarial training: a regularization method for supervised and semi-supervised learning. *IEEE transactions on pattern analysis and machine intelligence*, 41(8):1979–1993, 2018.
- [18] Sangwoo Mo, Minkyu Kim, Kyungmin Lee, and Jinwoo Shin. S-clip: Semi-supervised vision-language learning using few specialist captions, 2023.
- [19] Khanh-Binh Nguyen. Sequencematch: Revisiting the design of weak-strong augmentations for semi-supervised learning. In *Proceedings of the IEEE/CVF Winter Conference on Applications of Computer Vision (WACV)*, pp. 96–106, January 2024.
- [20] Khanh-Binh Nguyen. Debiasing, calibrating, and improving semi-supervised learning performance via simple ensemble projector. In *Proceedings of the IEEE/CVF Winter Conference on Applications of Computer Vision (WACV)*, pp. 2441–2451, January 2024.
- [21] Hieu Pham, Zihang Dai, Qizhe Xie, and Quoc V Le. Meta pseudo labels. In *Proceedings of the IEEE/CVF conference on computer vision and pattern recognition*, pp. 11557–11568, 2021.
- [22] Francois Porcher, camille couprie, Marc Szafraniec, and Jakob Verbeek. Better (pseudo-)labels for semi-supervised instance segmentation, 2024.
- [23] Alec Radford, Jong Wook Kim, Chris Hallacy, Aditya Ramesh, Gabriel Goh, Sandhini Agarwal, Girish Sastry, Amanda Askell, Pamela Mishkin, Jack Clark, et al. Learning transferable visual models from natural language supervision. In *International conference on machine learning*, pp. 8748–8763. PMLR, 2021.

- [24] Becca Roelofs, David Berthelot, Kihyuk Sohn, Nicholas Carlini, and Alex Kurakin. Adamatch: A unified approach to semi-supervised learning and domain adaptation. In *International Conference on Learning Representations (paper)*, 2022.
- [25] Swalpa Kumar Roy, Ali Jamali, Jocelyn Chanussot, Pedram Ghamisi, Ebrahim Ghaderpour, and Himan Shahabi. Simpoolformer: A two-stream vision transformer for hyperspectral image classification. *Remote Sensing Applications: Society and Environment*, pp. 101478, 2025.
- [26] Amir Hossein Saberi, Amir Najafi, Alireza Heidari, Mohammad Hosein Movasaghinia, Abolfazl Motahari, and Babak H. Khalaj. Out-of-domain unlabeled data improves generalization, 2024.
- [27] Kihyuk Sohn, David Berthelot, Nicholas Carlini, Zizhao Zhang, Han Zhang, Colin A Raffel, Ekin Dogus Cubuk, Alexey Kurakin, and Chun-Liang Li. Fixmatch: Simplifying semi-supervised learning with consistency and confidence. *Advances in neural information processing systems*, 33:596–608, 2020.
- [28] Nitish Srivastava, Geoffrey Hinton, Alex Krizhevsky, Ilya Sutskever, and Ruslan Salakhutdinov. Dropout: a simple way to prevent neural networks from overfitting. *The journal of machine learning research*, 15(1):1929–1958, 2014. Publisher: JMLR. org.
- [29] Takashi Takahashi. The role of pseudo-labels in self-training linear classifiers on high-dimensional gaussian mixture data, 2024.
- [30] Antti Tarvainen and Harri Valpola. Mean teachers are better role models: Weight-averaged consistency targets improve semi-supervised deep learning results. *Advances in neural information processing systems*, 30, 2017.
- [31] Sagar Vaze, Kai Han, Andrea Vedaldi, and Andrew Zisserman. Generalized category discovery. In *Proceedings of the IEEE/CVF Conference on Computer Vision and Pattern Recognition*, pp. 7492–7501, 2022.
- [32] Guanqun Wang, He Chen, Liang Chen, Yin Zhuang, Shanghang Zhang, Tong Zhang, Hao Dong, and Peng Gao. P²FEViT: Plug-and-play cnn feature embedded hybrid vision transformer for remote sensing image classification. *Remote Sensing*, 15(7):1773, 2023.
- [33] Yidong Wang, Hao Chen, Yue Fan, SUN Wang, Ran Tao, Wenxin Hou, Renjie Wang, Linyi Yang, Zhi Zhou, Lan-Zhe Guo, et al. Usb: A unified semi-supervised learning benchmark for classification. In *Thirty-sixth Conference on Neural Information Processing Systems Datasets and Benchmarks Track*, volume 35, pp. 3938–3961, 2022.
- [34] Yidong Wang, Hao Chen, Qiang Heng, Wenxin Hou, Yue Fan, , Zhen Wu, Jindong Wang, Marios Savvides, Takahiro Shinozaki, Bhiksha Raj, Bernt Schiele, and Xing Xie. Freematch: Self-adaptive thresholding for semi-supervised learning. In *International Conference on Learning Representations (paper)*, 2023.
- [35] Xianglei Xing, Yao Yu, Hua Jiang, and Sidan Du. A multi-manifold semi-supervised Gaussian mixture model for pattern classification. *Pattern Recognition Letters*, 34(16):2118–2125, 2013. ISSN 0167-8655. doi: <https://doi.org/10.1016/j.patrec.2013.08.005>. URL <https://www.sciencedirect.com/science/article/pii/S0167865513003000>.
- [36] Yi Xu, Lei Shang, Jinxing Ye, Qi Qian, Yu-Feng Li, Baigui Sun, Hao Li, and Rong Jin. Dash: Semi-supervised learning with dynamic thresholding. In *International conference on machine learning*, pp. 11525–11536. PMLR, 2021.
- [37] David Yarowsky. Unsupervised word sense disambiguation rivaling supervised methods. In *33rd annual meeting of the association for computational linguistics*, pp. 189–196, 1995.
- [38] Fisher Yu, Dequan Wang, Evan Shelhamer, and Trevor Darrell. Deep layer aggregation. In *Proceedings of the IEEE conference on computer vision and pattern recognition*, pp. 2403–2412, 2018.

- [39] Bowen Zhang, Yidong Wang, Wenxin Hou, Hao Wu, Jindong Wang, Manabu Okumura, and Takahiro Shinozaki. Flexmatch: Boosting semi-supervised learning with curriculum pseudo labeling. *Advances in Neural Information Processing Systems*, 34:18408–18419, 2021.
- [40] Bingchen Zhao, Xin Wen, and Kai Han. Learning semi-supervised gaussian mixture models for generalized category discovery. In *Proceedings of the IEEE/CVF International Conference on Computer Vision*, pp. 16623–16633, 2023.
- [41] Mingkai Zheng, Shan You, Lang Huang, Fei Wang, Chen Qian, and Chang Xu. Simmatch: Semi-supervised learning with similarity matching. In *Proceedings of the IEEE/CVF conference on computer vision and pattern recognition*, pp. 14471–14481, 2022.
- [42] Bo Zong, Qi Song, Martin Renqiang Min, Wei Cheng, Cristian Lumezanu, Daeki Cho, and Haifeng Chen. Deep Autoencoding Gaussian Mixture Model for Unsupervised Anomaly Detection. In *International Conference on Learning Representations*, 2018.